ISBN: 978-3-95450-248-6 ISSN: 2673-5490 doi: 10.18429/JACoW-IPAC2025-MOPB106

OPTIMIZING CHERENKOV WAVEGUIDE SEEDING FOR THz SASE FELs TOWARDS STABLE, FEW-CYCLE PULSES

K. Peetermans*, F. Lemery, Deutsches Elektronen-Synchrotron DESY, Hamburg, Germany
M. Krasilnikov, X. Li, Deutsches Elektronen-Synchrotron DESY, Zeuthen, Germany

Content from this work may be used under the terms of the CC BY 4.0 licence (© 2025). Any distribution of this work must maintain attribution to the author(s), title of the work, publisher, and DOI.

Abstract

The PITZ facility at DESY in Zeuthen has demonstrated the first operational high peak and average power THz self-amplified spontaneous emission (SASE) free electron laser (FEL). The current setup displays the onset of saturation at a central frequency of 3 THz using a 3.5 m long LCLS-I undulator. However, the THz user community has expressed the need for carrier-envelope phase (CEP) stability and the availability of few-cycle THz pulses to complement the currently demonstrated long pulses. In this work, simulations are conducted to evaluate and optimize FEL performance by incorporating a Cherenkov waveguide to seed the process. The waveguide parameter space is scanned to vary energy modulation depth and frequency, after which the performance is estimated using the space charge tracking algorithm, ASTRA, and the FEL simulation code, GENESIS1.3. The optimized parameters lead to a partially microbunched beam at the undulator entrance, allowing saturation to be reached much earlier. In the future, the implementation of such a scheme would facilitate generation of few-cycle, CEP-stable THz pulses to be used in user experiments.

INTRODUCTION

The PITZ accelerator consists of an L-band photocathode RF gun with a maximum cathode gradient of 60 MV/m, solenoids for emittance compensation, and an L-band booster cavity, which can accelerate the beam to a maximum momentum of 22 MeV/c. The booster is followed by detailed beam diagnostic devices, which measure the beam distribution, energy spectrum, and transverse and longitudinal phase spaces, etc. The EuXFEL user community has consistently expressed demand for high power THz sources [1], leading to a proof-of-concept THz experiment at PITZ. The photoinjector has been extended with one LCLS-I undulator to generate THz radiation [2, 3]. A chicane bunch compressor was installed before the undulator to allow generating beams with higher peak current or manipulating the longitudinal phase space of a prebunched beam. The layout of the main components for THz FEL is shown in Fig. 1.

To extend the parameter space of the THz pulses PITZ can produce, various methods of seeding the FEL are under investigation. In this work, a dielectric-lined waveguide (DLW) is inserted into the beam path, where the self-wake of the electron bunch will lead to an energy modulation within the bunch. A sketch is shown in Fig. 2. During the remaining transport towards the undulator, this modulation converts into a density modulation. If necessary, the chicane can also be used to increase the R_{56} of the transport. The current spikes that are produced this way can lase coherently in the undulator, therefore partially skipping the typical microbunching phase. THz pulses produced this way will achieve saturation sooner, meaning they will have a broader spectral content at the same energy. Depending on the application, such a pulse could be further compressed to improve performance.

Zhang *et al.* [4] simulated the use of a DLW at PITZ to modulate the beam upstream of the booster. Ma *et al.* [5] also explored the seeding of a THz undulator using laser-based modulation at the cathode. Building on Zhang's approach, this work focuses on optimizing the DLW parameters to improve THz FEL performance. Additionally, the DLW is now placed behind the booster, as it was established experimentally that beam transport using the previous configuration is challenging.

THEORY

An electron bunch passing through a DLW will excite a TM01 mode in the waveguide. With careful design of the structure parameters, the mode frequency falls in the THz regime. The characteristic equation is omitted here for brevity, but can be solved using ECHO1D [6, 7] to find the resonant frequency given the particle velocity v_p, dielectric permittivity e_r and inner- and outer radius a and $b = a+\delta$ of the dielectric. The mathematical expression of the wakefield, neglecting losses in the dielectric and the conductor, is of the form $w(s) = 2\kappa \cos(\omega_0 s/t)$, with κ the loss factor and s the distance to the generating particle. Particles following behind will lose or gain energy based on the relative distance, causing the electron bunch to have a self-induced energy modulation. At low energies (~ 17 MeV), the R_{56} of a drift of 20 m is approximately 0.018 m, meaning the ballistic bunching effect will suffice to convert this energy modulation into a considerable density modulation.

SIMULATION SETUP

Multiphysics start-to-end simulations of the PITZ beamline were performed using the simulation code ASTRA [8]. Starting from steady-state wake found using ECHO1D, the effect of a wake kick is implemented into the simulation. The program convolutes the Green's function with the charge density at a single point and evaluates the longitudinal wake force. Therefore, to simulate the effect of a beam travelling through the DLW for an extended period of time, the wake kicks are scaled down and applied every centimeter to produce a semi-continuous self-wake effect. The beam transport from the DLW to the undulator was optimized in OCELOT [9], following the method described in Ref. [10].

* karel.peetermans@desy.de

ISBN: 978-3-95450-248-6 ISSN: 2673-5490 doi: 10.18429/JACoW-IPAC2025-MOPB106

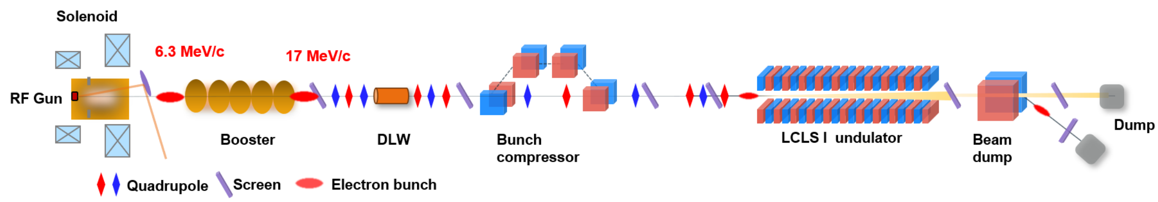

Figure 1: Schematic layout of the PITZ accelerator, marked with the position of the simulated DLW.

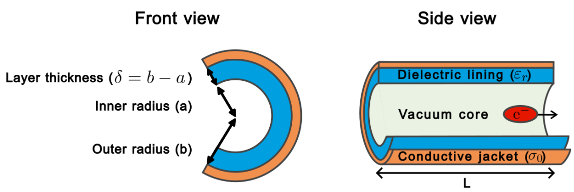

Figure 2: Sketch of a DLW and its parameters.

To investigate the influence of modulation depth and frequency, a parameter scan is performed over the layer thickness and length of the DLW. All parameter combinations are transported through the lattice optimized for δ = 200 µm and L = 10 cm, although in practice transport would have to be optimized for the specific parameter combination in question. Nonetheless, this method provides a realistic estimate of space-charge and transport effects. At entrance of the undulator, Twiss parameters are rescaled to match the optimized values to ensure transport through the undulator.

For each DLW parameter set, a GENESIS simulation of the LCLS-I undulator is performed following the method typically applied by the team at PITZ [3, 11]. GENESIS tracks slices of the bunch through the undulator, calculating the radiation produced and absorbed by each individual slice. It is typically used for frequencies in the X-ray regime. To apply this model in the THz range, where the wavelength is much longer, it is important that the current profile of the bunch is correctly represented within the slice. Within one wavelength, the current profile of a Gaussian bunch will have changed significantly more than for an x-ray wavelength. When implemented correctly, the local bunching amplitude of the slices will reflect that of the bunch realistically.

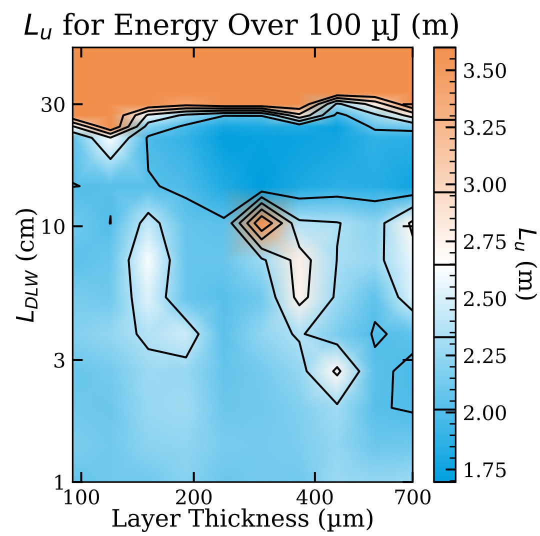

Figure 3: Heatmap of undulator length L_u required to reach 100 µJ. The minimum is found at L = 22 cm, δ = 237.5 µm.

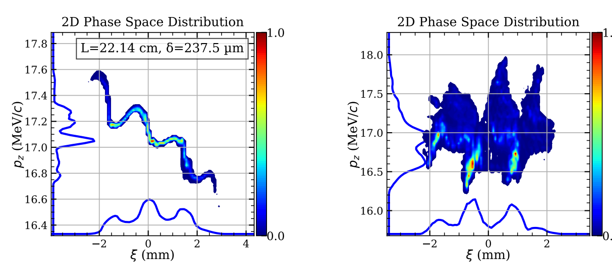

Figure 4: Best-case phase space for shortest undulator length to reach 100 µJ. Left: before lasing, right: after lasing. Particles in the left-most current spike lost up to 0.7 MeV.

SIMULATION RESULTS

A 2D heatmap of the undulator length required to produce a 100 µJ pulse is shown in Fig. 3. An optimal DLW length can be observed around L = 22 cm, where the undulator length goes down to around 1.8 m. For DLWs longer than ~ 25 cm, the length required increases sharply because of particle losses in the DLW. The focus at High1.Scr5 used in these simulations is quite narrow, and therefore does not allow structures of such length. For the L = 22 cm case, currently ~ 4% losses are observed and this can be further reduced with more precise optimization. At this length, the exact minimum undulator length l_u is found for δ = 237.5 µm, where l_u(100 µJ) = 1.71 m is found, compared to the unseeded result of 2.07 m. The phase space before and after lasing is shown in Fig. 4

This optimized case is now further compared to the unseeded simulation as well as the cold spot in the heatmap found at L = 10 cm and δ = 365.9 µm. This case is referred to as destructive seeding, because the specific parameter set has led to a lower saturation power than the non-seeded case. Figure 5 shows the energy gain along the undulator, indicating that initially, both seeded cases are gaining earlier than the unseeded bunch. The optimally seeded case however continues to an energy slightly higher than the unseeded case, E_{final} = 209.4 µJ vs. 207.7 µJ, while the destructively

Content from this work may be used under the terms of the CC BY 4.0 licence (© 2025). Any distribution of this work must maintain attribution to the author(s), title of the work, publisher, and DOI.

ISBN: 978-3-95450-248-6 ISSN: 2673-5490 doi: 10.18429/JACoW-IPAC2025-MOPB106

Content from this work may be used under the terms of the CC BY 4.0 licence (© 2025). Any distribution of this work must maintain attribution to the author(s), title of the work, publisher, and DOI.

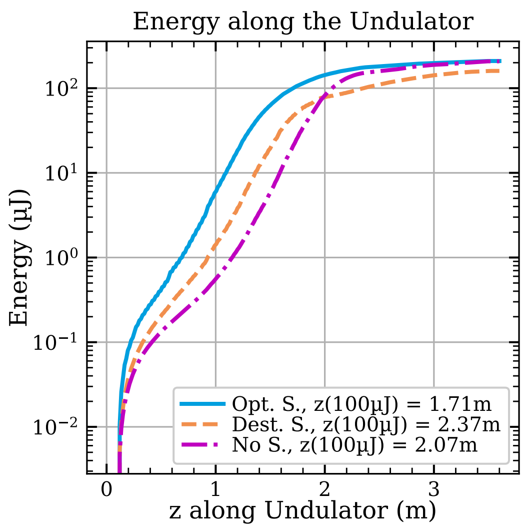

Figure 5: Energy gain curve for the three cases discussed in the text. In order of the legend these are: optimal seeding, destructive seeding and no seeding.

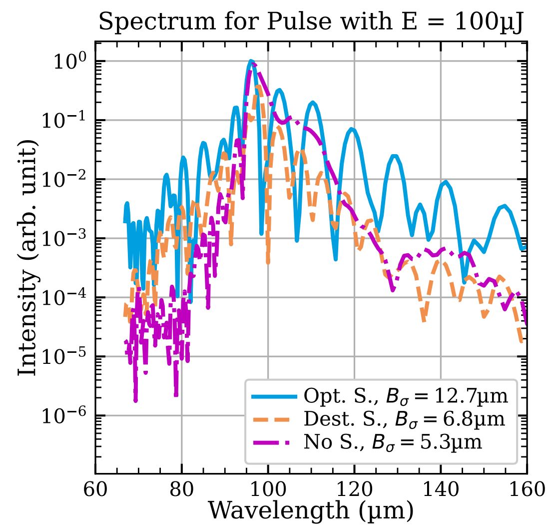

Figure 7: Intensity spectrum at $E = 100$ μJ. In order of the legend: optimal seeding, destructive seeding and no seeding. The optimally seeded case has more than double the bandwidth of the unseeded case.

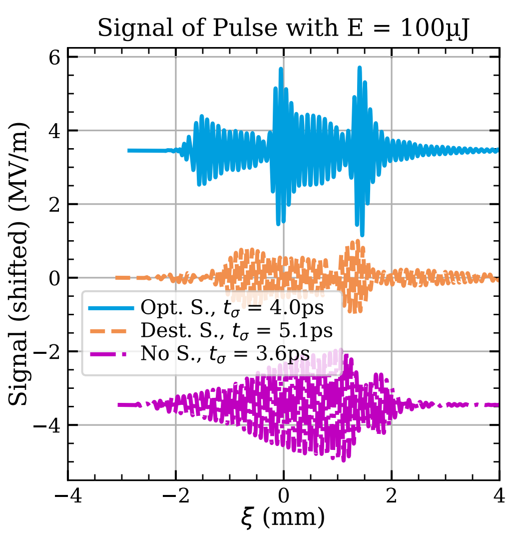

Figure 6: THz traces at $E = 100$ μJ. In order of the legend: optimal seeding, destructive seeding and no seeding.

seeded case only reaches 160 μJ. To further compare, the GENESIS output of the electric field is taken when the pulse has reached exactly 100 μJ. Fig. 6 shows the three THz pulses traces. Although the final pulse lengths are similar in all three cases, their intensity spectra differ significantly. This is shown in Fig. 7. The RMS bandwidth of the optimally seeded case ends up at 12.7 μm, which is more than double that of the unseeded case. This means that, after a pulse compression stage is applied, the peak power could be twice as high with half the pulse length.

CONCLUSION

In this work, the viability of DLW seeding of the THz SASE FEL was showcased in start-to-end simulations. The parameter space around ($L = 22$ cm, $\delta = 237.5$ μm) was shown to reduce the required undulator length down to 1.71 m; a 17% decrease from the unseeded case. The corresponding RMS bandwidth increase is roughly 240%.

Future work should identify the stability of the beam after leaving the DLW by evaluating the dipole kick related to beam position jitter. There are also several promising directions to improve seeding performance. Phase-space synthesis via non-uniform, 3D-printed DLWs could enable tailored energy modulations for different operational modes [12]. A higher-dimensional optimization algorithm could include not only the DLW parameters but also the optical elements of the beamline to provide the optimal phase-space at the undulator entrance. The current simulations did not incorporate a chicane, and its inclusion could enable further compression post-modulation or alternatively reduce the required length of the DLW. Overall, the results highlight a clear path forward toward seeding the FEL process using compact, waveguide-based pre-bunching schemes at PITZ.

ACKNOWLEDGEMENTS

This work was supported by funds of the European XFEL R&D program.

REFERENCES

[1] P. Zalden *et al.*, "Terahertz science at European XFEL", European XFEL, Tech. Rep. XFEL.EU TN-2018-001-01.0, 2016. `https://xfel.tind.io/record/1564`

ISBN: 978-3-95450-248-6 ISSN: 2673-5490 doi: 10.18429/JACoW-IPAC2025-MOPB106

[2] M. Krasilnikov *et al.*, "Experimentally minimized beam emittance from an *L*-band photoinjector", *Phys. Rev. Spec. Top. Accel Beams*, vol. 15, no. 10, p. 100 701, 2012. doi:10.1103/PhysRevSTAB.15.100701

[3] M. Krasilnikov *et al.*, "First high peak and average power single-pass THz free-electron laser in operation", *Phys. Rev. Accel. Beams*, vol. 28, no. 3, p. 030 701, 2025. doi:10.1103/PhysRevAccelBeams.28.030701

[4] X.-Y. Zhang, F. Lemery, M. Krasilnikov, P. Boonpornprasert, and X. Li, "Simulations of dielectric-lined waveguide seeding option for THz FEL at PITZ", in *Proc. IPAC'24*, Nashville, TN, USA, pp. 420–423, 2024. doi:10.18429/JACoW-IPAC2024-MOPG69

[5] S. Ma, H. Zhang, J. Pang, C. Liu, and Z. He, "Enhancement of chirped density modulation in electron beam for generating ultrashort THz radiation pulse", *Phys. Rev. Accel. Beams*, vol. 28, no. 4, p. 044 402, 2025. doi:10.1103/PhysRevAccelBeams.28.044402

[6] I. Zagorodnov and T. Weiland, "TE/TM field solver for particle beam simulations without numerical Cherenkov radiation", *Phys. Rev. Spec. Top. Accel. Beams*, vol. 8, no. 4, p. 042 001, 2005. doi:10.1103/PhysRevSTAB.8.042001

[7] I. Zagorodnov, *Echo2d - version 3.5*. https://echo4d.de/download/echo2d/

[8] K. Floettmann, *Astra a space tracking algorithm*, 2017. https://www.desy.de/~mpyflo/Astra_manual/Astra-Manual_V3.2.pdf

[9] I. Agapov, G. Geloni, S. Tomin, and I. Zagorodnov, "OCELOT: A software framework for synchrotron light source and FEL studies", *Nucl. Instrum. Methods Phys. Res., Sect. A*, vol. 768, pp. 151–156, 2014. doi:10.1016/j.nima.2014.09.057

[10] X. Li *et al.*, "Matching of a Space-Charge Dominated Beam into the Undulator of the THz SASE FEL at PITZ", in *Proc. IPAC'21*, Campinas, Brazil, May 2021, pp. 3244–3247. doi:10.18429/JACoW-IPAC2021-WEPAB257

[11] S. Reiche, *Genesis1.3, version 4*. https://github.com/svenreiche/Genesis-1.3-Version4

[12] F. Mayet, R. Assmann, and F. Lemery, "Longitudinal phase space synthesis with tailored 3D-printable dielectric-lined waveguides", *Phys. Rev. Accel. Beams*, vol. 23, no. 12, p. 121 302, 2020. doi:10.1103/PhysRevAccelBeams.23.121302

© Content from this work may be used under the terms of the CC BY 4.0 licence (© 2025). Any distribution of this work must maintain attribution to the author(s), title of the work, publisher, and DOI.